2008

Identification of factors limiting the critical current density in MgB2 _xCx superconductors at low magnetic fields

Olga V. Shcherbakova
University of Wollongong, olga@uow.edu.au

Alexey V. Pan
University of Wollongong, pan@uow.edu.au

Jianli Wang
University of Wollongong, jianli@uow.edu.au

Andrey Shcherbakov
University of Wollongong, as695@uow.edu.au

S. X. Dou
University of Wollongong, shi@uow.edu.au

See next page for additional authors

Publication Details

Shcherbakova, O. V., Pan, A. V., Wang, J., Shcherbakov, A., Dou, S. X. & Wexler, D. (2008). Identification of factors limiting the critical current density in MgB2 _xCx superconductors at low magnetic fields. In European Conference on Applied Superconductivity, 16-20 September, Brussels, Belgium. Journal of Physics, 97 012314-1-012314-6.

Identification of factors limiting the critical current density in $MgB_{2-x}C_x$ superconductors at low magnetic fields

O. V. Shcherbakova[1], A. V. Pan[1], J. L. Wang[1], A. V. Shcherbakov[1], S. X. Dou[1], D. Wexler[2]

[1] Institute for Superconducting and Electronic Materials, University of Wollongong, NSW 2522, Australia

[2]School of Materials, Mechanical and Mechatronic Engineering, University of Wollongong, NSW 2522, Australia

E-mail: os966@uow.edu.au (O. V. Shcherbakova)

Abstract. Structural analysis and electromagnetic measurements have been performed on a range of samples prepared by the liquid mixing approach to doping MgB_2 superconductor. The dopants used to enhance the current carrying ability of MgB_2 are sugar, malic acid, and polycarbosilane. The results obtained have allowed us to clarify the contributions of the factors limiting critical current at low magnetic fields in doped MgB_2.

1. Introduction

Extensive research on doping with different elements in MgB_2 superconductor, promising for high current applications, has revealed that carbon containing materials are the most effective for significant enhancement of the critical current density in high magnetic fields [1, 2, 3, 4]. This enhancement is mainly due to carbon (C) replacing boron (B) in the MgB_2 crystal lattice [5].

Recently the authors' group has reported a new advanced and, at the same time, simplified approach to the fabrication of C-doped MgB_2 superconductors. We have dissolved first sugar [6], and then other carbohydrates, such as malic acid [7] and polycarbosilane (PCS) [8], in an appropriate solvent (water [6] and toluene [7, 8]) and mixed it with boron powder. A reasonable assertion has been made [6] (and confirmed later [9]) that each boron particle becomes coated with a nano-layer of carbon after the mixture is dried. This offers the maximum surface and clean interfaces for reactions between the doping elements in the layer and the boron, as compared to the dry-mixed nano-powders. Importantly, the decomposition temperatures for the carbohydrates (sugar and malic acid, $< 200°C$ [6, 7]) and for polycarbosilane ($\sim 470°C$ [8]) are below the formation temperature of MgB_2 (650°C). Therefore, the carbon coating appears in a highly reactive (unpassivated) form when the MgB_2 formation reaction starts, promoting the enhanced incorporation of C in B sites in the MgB_2 lattice during the sintering [9].

The liquid mixing approach results in enhanced critical current density ($J_c(B_a)$) performance of the final $MgB_{2-x}C_x$ superconductors in high magnetic fields. Importantly, the J_c values at low fields were not degraded for sugar doping of up to 2.5 at.% [6] and for malic acid doping

of up to 30 wt.% [7]. This J_c behavior was presumed to occur due to the beneficial growth dynamics of MgB_2 and the absence of precipitates at the grain boundaries. However, higher levels of sugar (>8 at.%) and PCS doping (10 wt.%) attenuate the low field J_c performance of MgB_2 superconductor [6, 8].

The purpose of this work is to identify the factors limiting critical current density at low fields in $MgB_{2-x}C_x$ superconductors prepared by this advanced liquid mixing technique.

2. Experimental

$MgB_{2-x}C_x$ bulk samples have been prepared using a liquid mixing approach [6, 7]. To enable a comparative analysis, three dopants: sugar ($C_6H_{12}O_6$), malic acid (malic later in the text) ($C_4H_6O_5$), and polycarbosilane (C_2H_6Si) were added at the level of 10 wt%. After the liquid mixing stage, the samples were prepared in a similar way to that described in Ref. [8]. The samples were heated at the rate of 5°C/min and sintered at 700 and 900°C for 30 min, followed by furnace cooling to room temperature.

Phase analysis was performed with help of X-ray diffraction (XRD). The fractions of phases, as well as the lattice parameters were estimated via Rietveld refinement of XRD patterns. The structural features of samples were investigated by Scanning Electron Microscopy (SEM) and Transmission Electron Microscopy (TEM). The $J_c(B_a)$ curves were derived from the height of the magnetization loops measured in fields of up to 8 T, using the critical state model.

3. Results and discussion

The structures obtained from SEM and TEM are presented in Fig. 1. The results show:
(i) Grain size varies within each sample and depends on the different doping materials [Fig. 1]. The grains range from spheroids $\sim$ 20 nm in size (solid arrows) to large grains elongated in one direction (dotted arrows). The elongated grains are up to 50 nm×400 nm in the pure samples [Fig. 1(a,b)] and 80 nm×900 nm in the malic-doped samples [Fig. 1(c,d)]. In the sugar [6] and PCS-doped samples the maximum grain size is about 50 nm×150 nm [Fig. 1(e,f)].

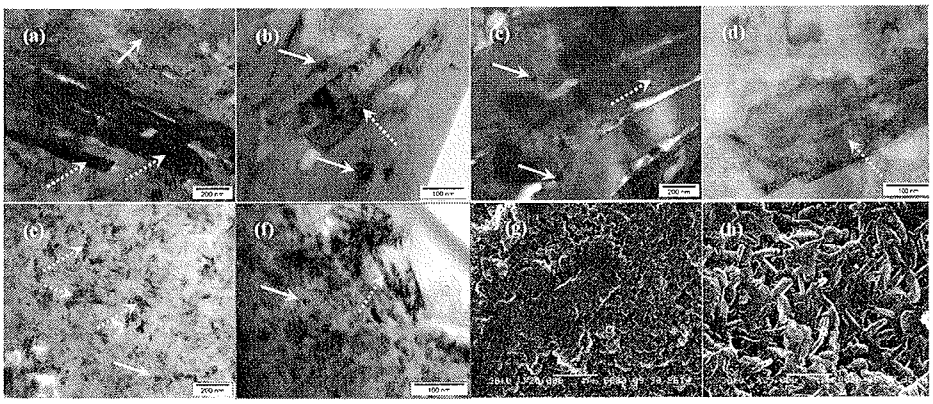

Figure 1. TEM investigation of grain boundaries in pure (a, b), 10 wt.% malic (c, d), and 10 wt.% PCS-doped MgB_2 (e, f). Typical SEM microstructure for malic and sugar (shown) doped MgB_2 synthesized at 700 °C (g) and 900 °C (h).

(ii) Typical structural defects are stacking faults, dislocations and nano-domains (< 20 nm) [9]. In the doped samples, denser networks of defects form because C-substitution promotes stronger crystal lattice distortion (large Δa and x values in Table 1).

(iii) MgO impurities are found in *all* samples. The level of MgO phase increases from pure (7.81 wt.%) and PCS doped (7.62 wt.%) to malic (11.7 wt.%) and sugar (17.9 wt.%) doped MgB_2.
(iv) Mg_2Si nano-precipitates with a diameter of < 20 nm are presented in the PCS-doped samples within MgB_2 grains . The level of Mg_2Si phase is 11.2 wt.%.
(v) The level of porosity (voids) varies considerably. The pure sample has $\sim$ 17% porosity of the studied area, which is lower than reported previously [22], but it is a non-typical result for our samples. The doped samples have higher levels of porosity: 25%, 37%, and 42% for malic, PCS, and sugar dopants, respectively.

Table 1. Some parameters of the samples prepared at 700°C. Lattice parameter a is defined from XRD patterns; $\triangle a$ defines changes in the a lattice parameter as a result of C incorporated into the MgB_2 lattice on B sites. The amount of C substituted for B is defined as x, which has been estimated from the neutron diffraction data of Ref. [11]. A_{eff} is the proportion of cross-sectional area that is electrically connected.

Dopant	a, nm	$\triangle a$, nm	x in $MgB_{2-x}C_x$	J_c(0T, 20K), $\times 10^9$ A/m^2	ρ_{40K}, $\mu\Omega cm$	ρ_{300K}, $\mu\Omega cm$	A_{eff}
none	3.0844	-	-	4.0	40	86	0.160
malic	3.0749	0.009	0.031	3.4	106	194	0.138
PCS	3.0741	0.010	0.033	2.8	198	289	0.137
sugar	3.0716	0.012	0.037	2.0	193	295	0.130

The liquid mixing ultimately results in the significant enhancement of the $J_c(B_a)$ performance for all the dopants [Fig. 2(a,b)], which is consistent with our previous results [6, 7]. The high field $J_c(B_a)$ performance seems to be rather well understood in the literature [2, 5, 19, 20]. Here, we mainly focus on the low field region. A considerable degradation of J_c in small fields has been observed for C-containing dopants [2, 4, 13]. This is not always the case for samples fabricated by liquid mixing as can be seen in Fig. 2 and Refs. [6, 7]. The following factors may be crucial for J_c behavior at low fields: *porosity* and *the amount of impurity phases* ("geometrical" factor), and the *connectivity of grain boundaries* [13, 14, 18, 21, 22]. Below, we suggest a simple

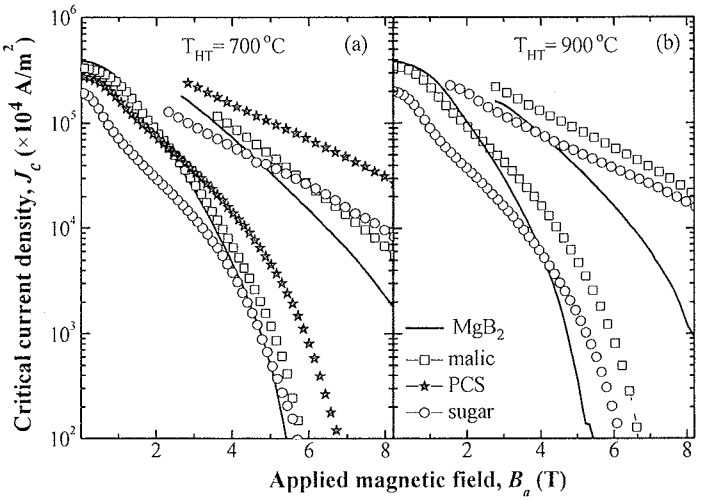

Figure 2. The $J_c(B_a)$ performance of MgB_2 with different dopants that was sintered at 700°C (a) and 900°C (b). The results on malic doping at 900°C are from Ref. [7]. The pure MgB_2 was prepared without employing liquid mixing.

consideration, which enables us to clarify the $J_c(B_a)$ behaviour at low fields.

First, we take into account the effect of the "geometrical" factor of the microstructure on J_c degradation at low fields. We have recalculated the measured critical current density (J_c^{meas}), assuming that the supercurrent flows only through the superconductor, so that the cross-sectional area for the current flow can be reduced by subtracting the non-superconducting fraction occupied by "geometrical" defects (A_g) [see (iii), (iv) and Table 1]. Accordingly, the critical current density of the sample fraction which is free from "geometrical" defects can be estimated as follows:

$$J_c^{geom} = J_c^{meas} \times \frac{A}{A - A_g} = J_c^{meas} \times \frac{1}{1 - A_g/A} \tag{1}$$

where A is the total cross-sectional area and $(1 - A_g/A)$ is the fraction of superconducting sample which is free from "geometrical" defects (for more details see Ref. [9]).

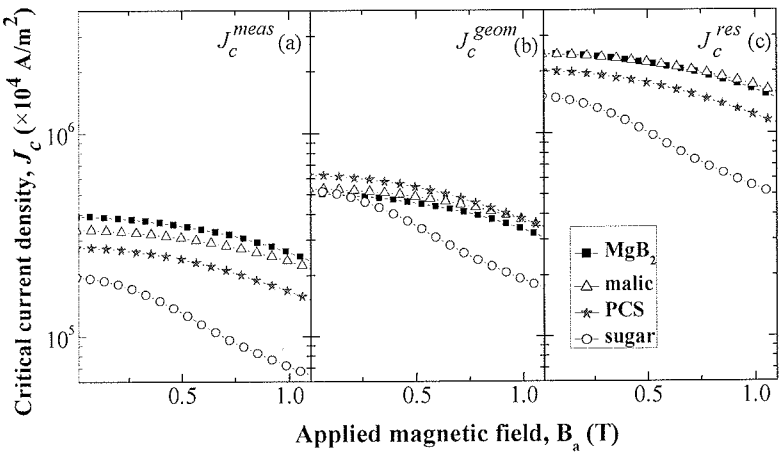

Figure 3. The low field part of J_c as measured (a), recalculated considering porosity and superconducting volume (b), and connectivity (c) for the samples studied.

The resultant J_c^{geom} adjustment for porosity and non-superconducting phase at low B_a is shown in Fig. 3(b). It turns out that almost all the samples show similar $J_c^{geom}(B_a \to 0)$ behaviour. The sample with sugar doping shows slightly different behaviour at $B_a > 0.25$ T, which is similar to the $J_c(B_a \to 0)$ performance observed in samples with pronounced weak links between the grains [22]. Indeed, the sugar doped sample has the highest level of MgO impurities among the samples studied [see (iii)]. It is likely that at this high level ($\sim 18\%$) a considerable part of these impurities resides not only inside the grains, but also on the grain boundaries. In this case they act as weak links, significantly reducing the connectivity and transparency of grain boundaries for current flow.

Generally, the higher the impurity content, the lower the J_c is at small B_a [Table I, (iii), (iv)]. Indeed, the transparency of the boundaries in the pure MgB_2 is reduced due to MgO impurities distributed in between and within MgB_2 grains in the form of nano-Mg(B, O)$_2$ precipitates, amorphous layers of BO_x, and so on [19, 15, 16, 17]. Additional impurities in doped samples clearly would attenuate the transparency of the boundaries, so that $J_c(0)$ is well below the attainable depairing current density $\sim 10^{12}$ A/m^2 [23].

The connectivity of grain boundaries is the *second* factor to take into account. We have employed semiquantitative Rowell analysis [25] to estimate the effective cross-section

of electrically connected area A_{eff} in the samples [Table 1]. According to Ref. [25], $A_{eff} = \Delta\rho_{ideal}/\Delta\rho$, where $\Delta\rho = \rho_{300K} - \rho_{40K}$ for the sample and $\Delta\rho_{ideal}$ is the value that would be obtained in a fully connected sample. For MgB_2, the $\Delta\rho_{ideal}$ value has been assumed to be 7.3 $\mu\Omega$cm for a dense MgB_2 filament made by chemical vapor deposition (CVD) [26]. For carbon-doped samples, $\Delta\rho_{ideal}(x)$ values have been estimated according to equation $\Delta\rho_{ideal}(x) = 109.59x + 8.8794$ [27] (where x is the level of C-substitution in the lattice), taken empirically from the data on CVD-made fully connected $MgB_{2-x}C_x$ wires. Similarly to Eq.(1), $J_c^{res} = J_c^{meas} \times \frac{1}{A_{eff}}$. The resultant J_c^{res} adjustment for connectivity is shown in Fig. 3(c).

As can be seen, the malic doping results in $J_c^{res}(B_a \rightarrow 0)$ similar to that of pure MgB_2 [Fig. 3(c)], despite the fact that the doped sample has a higher impurity level than the pure sample. The most obvious difference between all these samples is the size of their grains [Fig. 1(a-d)]. The malic-doped sample, having the largest grains [Fig. 1(c,d)], exhibits the highest J_c at low fields compared to all the other doped samples, having much smaller grains. Therefore, fewer boundaries having minimal scattering (i.e. higher overall transparency), is likely to be the key to larger J_c at low fields for the malic-doped samples. The reason for large grain formation in malic-doped samples is still unclear. It could be due to a catalytic effect of this dopant during the sintering. A similar grain size influence could be expected for sugar doping. However, the presence of a large amount of oxygen in sugar, leading to a significant amount of impurities, is likely to result in numerous grain nucleation and different grain formation dynamics for relatively large doping levels, when conpared to the malic-doped samples. In addition, the higher level of non-superconducting impurities in PCS and sugar doped samples [see (iii), (iv)] is another reason for increased scattering and, hence, current dissipation, which results in notable decrease of J_c^{res} values at $B_a \rightarrow 0$ [Fig. 3(c)].

One could try to increase the grain size in the samples, for example, by slower cooling rates [14] or increasing the sintering temperature [Fig. 1(g,h)]. The $J_c(B_a)$ performance of our samples undergoes significant enhancement over the entire field range for the samples sintered at 900°C compared to 700°C [Fig. 2(a,b)]. However, the $J_c(0)$ value is only slightly increased for samples sintered at 900°C. This suggests that the grain boundaries are exposed to a higher degree of contamination with oxide and doping sub-products at higher temperatures, which leads to a reduced transparency, limiting J_c, *particularly* at low fields. However, the substitution and pinning are enhanced as indicated by large J_c at high fields.

The $J_c(B_a)$ enhancement in the doped MgB_2 samples at high fields has been widely discussed [1, 2, 14, 19]. The commonly identified pinning types induced by doping are "secondary" *crystal lattice defects* produced by C-substitution and *nano-scale impurities*. Additionally, we should point out the generally overlooked fact that a broader range of various pinning sites can be involved in pinning in the doped samples. Indeed, the higher scattering in the doped samples leads to a reduced coherence length (ξ), as is evident from the considerably higher second critical fields B_{c2} [3, 10, 20, 24]. As a result, smaller size defects (e.g. strain fields in the crystal lattice around substitution sites with a reduced superconducting order parameter), which are less effective for pure samples with larger ξ, become pinning sites. This can explain the stronger enhancement for the doped samples at lower temperatures [Fig. 2(a,b)] at which $\xi(T)$ is the smallest.

4. Conclusion

A comparative structural and electromagnetic analysis of $MgB_{2-x}C_x$ samples prepared by a liquid mixing approach and with different doping materials (malic acid, sugar, PCS) has allowed us to establish the main factors limiting J_c, particularly at low fields. They include porosity, impurities, grain size, and transparency of the grain boundaries. According to the results of this work, an "ideal" (guiding) recipe for the J_c enhancement over the entire field region for MgB_2 superconductors is to create a dense single-crystalline structure with a maximum density

of ξ-scale pinning sites, yet allowing maximum supercurrent flow transparency. It is the same recipe as for HTS films and coated conductors. The practical guide for MgB_2 can be sought in careful consideration of the relevant factors discussed in our paper.

Acknowledgments

The authors would like to thank S. Zhou, M. S. A. Hossain, and T. Silver for fruitful discussions. The work is financially supported by the Australian Research Council.

References

[1] Dou S X, Pan A V, Zhou S, Ionescu M, Liu H K and Munroe P R 2002 *Supercond. Sci. Technol.* **15** 1587

[2] Dou S X, Pan A V, Zhou S, Ionescu M, Wang X L, Horvat J, Liu H K and Munroe P R 2003 *J. Appl. Phys.* **94** 1850

[3] Wilke R H T, Bud'ko S L, Canfield P C, Finnemore D K, Suplinskas R J and Hannahs S T 2004 *Phys. Rev. Lett.* **92** 217003

[4] Yamamoto A, Shimoyama J, Ueda S, Iwayama I, Horii S and Kishio K 2005 *Supercond. Sci. Technol.* **18** 1323

[5] Mazin I I, Andersen O K, Jepsen O, Dolgov O V, Kortus J, Golubov A A, Kuz'menko A B and D. van der Marel 2002 *Phys. Rev. Lett.* **89** 107002

[6] Zhou S, Pan A V, Wexler D and Dou S X 2007 *Adv. Mater.* **19** 1373

[7] Kim J H, Zhou S, Hossain M S A, Pan A V and Dou S X 2006 *Appl. Phys. Lett.* **89** 142505

[8] Shcherbakova O V, Pan A V, Wexler D and Dou S X, 2007 *IEEE Trans. Appl. Supercond.* **17** 2790

[9] Shcherbakova O V et al., in preparation.

[10] Dou S X, Braccini V, Soltanian S, Klie R, Zhu Y, Li S, Wang X L and Larbalestier D 2004 *J. Appl. Phys.* **96** 7549

[11] Avdeev M, Jorgensen J D, Ribeiro R A, Bud'ko S L and Canfield P C 2003 *Physica C* **387** 301

[12] Yeoh W K, Kim J H, Horvat J, Xu X, Qin M J, Dou S X, Jiang C H, Nakane T, Kumakura H and Munroe P 2006 *Supercond. Sci. Technol.* **19** 596

[13] Shcherbakova O, Dou S X, Soltanian S, Wexler D, Bhatia M, Sumption M and Collings E W 2006 *J. Appl. Phys.* **99** 08M510

[14] Shcherbakova O V, Pan A V, Soltanian S, Dou S X and Wexler D 2007 *Supercond. Sci. Technol.* **20** 5

[15] Liao X Z, Serquis A, Zhu Y T, Huang J Y, Civale L, Peterson D E, Mueller F M and Xu H F 2003 *J. Appl. Phys.* **93** 6208

[16] Klie R F, Idrobo J C, Browning N D, Regan K A, Rogado N S and Cava R J 2001 *Appl. Phys. Lett.* **79** 1837

[17] Klie R F, Idrobo J C, Browning N D, Serquis A, Zhu Y T, Liao X Z and Mueller F M 2002 *Appl. Phys. Lett.* **80** 3970

[18] Braccini V, Applied Superconductivity Conference 2006, Seattle, USA, 27 August - 1 September 2006.

[19] Serquis A, Liao X Z, Zhu Y T, Coulter J Y, Huang J Y, Willis J O, Peterson D E, Mueller F M, Moreno N O, Thompson J D, Nesterenko V F and Indrakanti S S 2002 *J. Appl. Phys.* **92** 351

[20] Matsumoto A, Kumakura H, Kitaguchi H, Senkowicz B J, Jewell M C, Hellstrom E E, Zhu Y, Voyles P M and Larbalestier D C 2006 *Appl. Phys. Lett.* **89** 132508

[21] Polyanskii A, Beilin V, Felner I, Tsindlekht M I, Yashchin E, Dul'kin E, Galstyan E, Roth M, Senkowicz B and Hellstrom E 2004 *Supercond. Sci. Technol.* **17** 363

[22] Pan A V, Zhou S, Liu H and Dou S 2003 *Supercond. Sci. Technol.* **16** 639

[23] Finnemore D, Ostenson J E, Bud'ko S L, Lapertot G and Canfield P C 2001 *Phys. Rev. Lett.* **86** 2420

[24] Sumption M D, Bhatia M, Rindfleisch M, Tomsic M, Soltanian S, Dou S X and Collings E W 2005 *Appl. Phys. Lett.* **86** 092507

[25] Rowell J M, 2003 *Supercond. Sci. Technol.* **16** R17

[26] Canfield P C, Finnemore D K, Budko S L, Ostenson J E, Lapertot G, Cunningham C E and Petrovic C 2001 *Phys. Rev. Lett.* **86** 2423

[27] Senkowicz B J, Polyanskii A, Mungall R J, Zhu Y, Giencke J E, Voyles P M, Eom C B, Hellstrom E E and Larbalestier D C 2007 *Supercond. Sci. Technol.* **20** 650